

Robust fractionation in cancer radiotherapy

Ali Ajdari, Archis Ghate

January 20, 2016

Abstract

In cancer radiotherapy, the standard formulation of the optimal fractionation problem based on the linear-quadratic dose-response model is a non-convex quadratically constrained quadratic program (QCQP). An optimal solution for this QCQP can be derived by solving a two-variable linear program. Feasibility of this solution, however, crucially depends on the so-called alpha-over-beta ratios for the organs-at-risk, whose true values are unknown. Consequently, the dosing schedule presumed optimal, in fact, may not even be feasible in practice. We address this by proposing a robust counterpart of the nominal formulation. We show that a robust solution can be derived by solving a small number of two-variable linear programs, each with a small number of constraints. We quantify the price of robustness, and compare the incidence and extent of infeasibility of the nominal and robust solutions via numerical experiments.

1 Background and motivation

The goal in external beam radiotherapy for cancer is to maximize damage to the tumor while limiting toxic effects of radiation on nearby organs-at-risk (OAR). Treatment is typically delivered over multiple treatment sessions called fractions. This leads to a well-known optimization problem, often referred to as the *fractionation problem*. The goal in this problem is to find the number of fractions N and a corresponding sequence $\vec{d} = (d_1, d_2, \dots, d_N)$ of doses so as to maximize tumor-damage while ensuring that the OAR can safely tolerate these doses. The fundamental tradeoffs in this problem are as follows. Normal-cells often have a better damage-repair capability than tumor-cells. Temporal dispersion of dose across multiple fractions thus gives the OAR time to recover between sessions. For most tumors, a large number of fractions with a small dose per fraction allows the treatment planner to inflict more damage on the tumor as compared to administering a small number of fractions with a large dose per fraction. However, tumors can proliferate over the treatment course, and thus a shorter course might work better as it kills the tumor before any significant proliferation. Thus the question is whether or not and how the treatment planner can exploit, for patients' benefit, the differences in the way in which tumors and OAR respond to radiation.

1.1 Mathematical formulations of the fractionation problem

The fractionation problem has been studied extensively, both clinically and mathematically, for over a century [22]. Mathematical formulations of this problem routinely rely on the linear-quadratic (LQ) cell-survival model [14]. Key parameters of the LQ model include the so-called α/β ratios for the OAR. Research that uses this LQ model has evolved from single-OAR formulations, to two-OAR formulations, and, more recently, to models with multiple OAR. All of these formulations belong to the class of non-convex quadratically constrained quadratic programs (QCQPs) — problems known

to be computationally difficult in general. A closed-form optimal solution is available for the single OAR case (see, for example, [7, 12, 13, 15, 20, 28] and references therein). One paper provided an optimal dosing scheme using Karush-Kuhn-Tucker conditions for the two-OAR case for a fixed N [5]. A simulated annealing heuristic was applied to a two-OAR formulation in [29].

The most recent multiple-OAR formulation of this problem (see [24, 26]) is given by

$$\text{(FRAC)} \quad \max_{\vec{d}, N} \quad \alpha_0 \sum_{t=1}^N d_t + \beta_0 \sum_{t=1}^N d_t^2 - \tau(N) \quad (1)$$

$$\sum_{t=1}^N d_t + \rho_m \sum_{t=1}^N d_t^2 \leq \text{BED}_m, \quad m \in \mathcal{M}, \quad (2)$$

$$\vec{d} \geq 0, \quad (3)$$

$$1 \leq N \leq N_{\max}, \text{ integer.} \quad (4)$$

In this problem, α_0, β_0 are the tumor's dose-response parameters as per the LQ model. The term $\tau(N)$ in the objective function accounts for tumor proliferation and is given by

$$\tau(N) = \frac{[(N-1) - T_{\text{lag}}]^+ \ln 2}{T_{\text{double}}}, \quad (5)$$

where $[(N-1) - T_{\text{lag}}]^+$ is defined as $\max\{0, (N-1) - T_{\text{lag}}\}$. Here, T_{lag} is the time-lag (in days) after which tumor proliferation starts after treatment initiation; and T_{double} (in days) denotes the doubling time for the tumor. This proliferation term assumes that a single fraction is administered every day; it can be generalized to accommodate other fractionation schemes as described in [24]. The objective function equals the biological effect (BE) of \vec{d} on the tumor, which is to be maximized. In constraints (2), $\mathcal{M} = \{1, 2, \dots, n\}$ is the set of $n \geq 1$ OAR. The parameter $\rho_m = \beta_m/\alpha_m$ is the aforementioned (inverse) ratio of dose-response parameters for OAR $m \in \mathcal{M}$. The left hand side of each constraint equals the biologically effective dose (BED) administered to the corresponding OAR. The term on the right hand side is given by $\text{BED}_m = D_m + \rho_m D_m^2/N_m$. It equals the BED of a conventional treatment schedule that administers a total dose of D_m in N_m equal-dosage fractions and that OAR m is known to tolerate. Thus, each of these constraints ensures that, for each OAR, the BED of \vec{d} is no more than what is safe for that OAR. In constraint (4), N_{\max} is the maximum number of fractions that is logistically feasible in the treatment protocol. In the sequel, we will often refer to (FRAC) as the nominal problem.

1.2 Optimal solution of the nominal fractionation problem

An optimal solution for this multiple-OAR case was provided in [24]; this solution works either when $\alpha_0/\beta_0 \leq \min_{m \in \mathcal{M}} (\alpha_m/\beta_m)$ or when $\alpha_0/\beta_0 \geq \max_{m \in \mathcal{M}} (\alpha_m/\beta_m)$. The first provably optimal solution that works irrespective of the ordering of these ratios for the multiple-OAR case was recently derived in [26] based on the doctoral dissertation of Saberian [23]. This solution was obtained by equivalently reformulating (FRAC) for each fixed N as a *two-variable* linear program (LP) with $n+2$ linear constraints and non-negativity constraints on the two variables. The two variables in this LP are

$$x = \sum_{t=1}^N d_t \quad \text{and} \quad y = \sum_{t=1}^N d_t^2 \quad \text{and the LP is given by}$$

$$\text{(2VARLP)} \quad \max_{x,y} \quad \alpha_0 x + \beta_0 y - \tau(N) \quad (6)$$

$$x + \rho_m y \leq \text{BED}_m, \quad m \in \mathcal{M}, \quad (7)$$

$$y \leq \gamma^* x, \quad (8)$$

$$c^* x \leq y, \quad (9)$$

$$x \geq 0, \quad (10)$$

$$y \geq 0, \quad (11)$$

where $\gamma^* = \min_{m \in \mathcal{M}} b_m(1)$ and $c^* = \min_{m \in \mathcal{M}} b_m(N)$ with $b_m(N) = \frac{-1 + \sqrt{1 + 4\rho_m \text{BED}_m / N}}{2\rho_m}$ for $m \in \mathcal{M}$ and for all $N \geq 1$. Specifically, for each fixed N , if x^* , y^* is an optimal solution of this LP, then the dosing schedule $(q, \underbrace{p, p, \dots, p}_{N-1 \text{ times}})$, where

$$p = \frac{x^*}{N} \left[1 - \sqrt{1 - \left(1 - \frac{y^*}{(x^*)^2} \right) \left(\frac{N}{N-1} \right)} \right], \quad (12)$$

$$q = x^* - (N-1)p, \quad (13)$$

is optimal. Moreover, it can be shown that there are only three possibilities for x^* and y^* . The first is where $\sqrt{y^*} = x^*$ and then $p = 0$ (this is called a single-dosage solution); the second is where $\sqrt{N}y^* = x^*$ and then $p = q$ (this is called an equal-dosage solution); and the third is where $\sqrt{y^*} < x^* < \sqrt{N}y^*$ and then $0 \neq p \neq q \neq 0$ (this is called an unequal-dosage solution) (see [23, 26] for details). An optimal number of fractions can then be found by substituting a dosing schedule so obtained into the objective function in (FRAC) for each $N \in \{1, 2, \dots, N_{\max}\}$ and picking the one that yields the largest tumor BE. Consequently, (FRAC) is solved by solving exactly N_{\max} two-variable LPs.

1.3 Limitations of existing formulations and our contributions

One drawback of all aforementioned formulations of the fractionation problem based on the LQ model is that the values of ρ_m are not known. Thus, a dosing schedule derived using estimated or “nominal” values of these parameters may not even be feasible in practice.

In a recent unpublished manuscript [2], Badri et al., independently of an earlier (May 2015) unpublished version of our present work, attempted to remedy this by studying a robust formulation of the above fractionation problem. In their formulation, the treatment planner derives a robust solution by assuming that the ρ_m values vary within a known non-negative interval. However, the crucial dependence of the right hand side BED_m on ρ_m in constraints (2) was ignored in that manuscript. This meant that an optimal solution to their robust formulation was obtained by replacing ρ_m on the left hand side in (2) by its largest possible value. This implied that the robust solution is derived simply by solving the two-variable LP in [23, 26]. Unfortunately, since the right hand side in constraints (2) in fact explicitly depends on ρ_m , such a simplified solution might not be robust in practice. Badri et al. rectified this limitation in an updated unpublished variation [1] of their original manuscript, again independently of the earlier (May 2015) unpublished version of our present work that they cited.

The main focus of the original and the updated versions by Badri et al. was on a chance constrained formulation of the problem, which required the treatment planner to know the probability distribution of alpha-over-beta ratios, and which called for a computationally more demanding solution approach than what is needed for the robust formulation. On the plus side, a potential benefit of the resulting chance constrained solution is that it might be less conservative than the robust solution (although this is perhaps impossible to verify rigorously). Given their alternative focus,

Badri et al. gave a somewhat cursory treatment to the robust approach in both their manuscripts, did not present an infeasibility analysis of the resulting robust solutions, did not quantify the price of robustness, and only included minimal sensitivity results.

Here we study essentially the same robust problem as in the updated version of Badri et al. We do, however, provide mathematical and clinical insights missing in their work. Firstly, we present our solution approach in much more detail. We show that, for each fixed N , an optimal solution to the non-convex robust problem can be recovered by solving $n + 1$ two-variable LPs. Consequently, the robust fractionation problem is solved by solving $(n + 1)N_{\max}$ two-variable LPs; each of these LPs includes $n + 2$ linear constraints and non-negativity constraints on the two variables. We perform sensitivity analyses with respect to the values of T_{lag} and T_{double} currently available in the clinical literature to numerically quantify the price of robustness. We also provide qualitative and quantitative comparisons between the nominal and robust fractionation schedules. Finally, we present an extensive analysis of the infeasibility suffered by the nominal and robust solutions in a broad range of scenarios.

This paper is organized as follows. Our robust formulation is described in the next section. The solution approach is detailed in Section 3. Numerical results are presented in Section 4. We conclude with a summary of our contributions, an outline of some variations and limitations of our model, and opportunities for future work.

2 A robust formulation

We refer the reader to [3] for a textbook and to [4] for a survey on robust optimization. We employ a standard interval uncertainty model from these existing works to construct a robust counterpart of the nominal problem (FRAC). Specifically, we use $\tilde{\rho}_m$ to denote the “true” unknown value of ρ_m , for $m = 1, \dots, n$. We assume that this unknown value belongs to a known interval of values $[\rho_m^{\min}, \rho_m^{\max}]$; here $0 < \rho_m^{\min} \leq \rho_m^{\max} < \infty$. We wish to find an N, \vec{d} pair that is feasible to BED constraints (2) for all $m \in \mathcal{M}$ no matter what true values $\tilde{\rho}_m$ are realized (as long as they belong to the aforementioned intervals). The resulting robust counterpart of (FRAC) is given by

$$\max_{\vec{d}, N} \alpha_0 \sum_{t=1}^N d_t + \beta_0 \sum_{t=1}^N d_t^2 - \tau(N) \quad (14)$$

$$\sum_{t=1}^N d_t + \tilde{\rho}_m \left(\sum_{t=1}^N d_t^2 - \frac{D_m^2}{N_m} \right) \leq D_m, \quad m \in \mathcal{M}, \quad \forall \tilde{\rho}_m \in [\rho_m^{\min}, \rho_m^{\max}], \quad (15)$$

$$\vec{d} \geq 0, \quad (16)$$

$$1 \leq N \leq N_{\max}, \text{ integer}. \quad (17)$$

Note here that, for simplicity of exposition, our formulation does not consider uncertainty in the values of α_0 and β_0 for the tumor. It is standard in robust optimization to not include uncertainty in the objective function coefficients. Uncertainty in these tumor parameters can, however, be easily incorporated by maximizing the worst-case value of the objective function (we accomplish this in our numerical results in Section 4.3).

By introducing $\rho_m^{\text{mean}} = (\rho_m^{\max} + \rho_m^{\min})/2$ and $\rho_m^{\text{range}} = (\rho_m^{\max} - \rho_m^{\min})/2$, and after some simple algebra, we can see that for each OAR $m \in \mathcal{M}$, constraint 15 is equivalent to the following constraint:

$$\sum_{t=1}^N d_t + \rho_m^{\text{mean}} \sum_{t=1}^N d_t^2 + \rho_m^{\text{range}} \left| \sum_{t=1}^N d_t^2 - \frac{D_m^2}{N_m} \right| \leq D_m + \rho_m^{\text{mean}} \frac{D_m^2}{N_m}. \quad (18)$$

Thus, by defining the shorthand notation $\text{RC}_m = D_m + \rho_m^{\text{mean}} \frac{D_m^2}{N_m}$, and putting the above pieces together, we can rewrite the robust counterpart (14)-(17) as

$$\text{(RFRAC)} \quad f^* = \max_{\vec{d}, N} \alpha_0 \sum_{t=1}^N d_t + \beta_0 \sum_{t=1}^N d_t^2 - \tau(N) \quad (19)$$

$$\sum_{t=1}^N d_t + \rho_m^{\text{mean}} \sum_{t=1}^N d_t^2 + \rho_m^{\text{range}} \left| \sum_{t=1}^N d_t^2 - \frac{D_m^2}{N_m} \right| \leq \text{RC}_m, \quad m \in \mathcal{M}, \quad (20)$$

$$\vec{d} \geq 0, \quad (21)$$

$$1 \leq N \leq N_{\max}, \text{ integer}. \quad (22)$$

As in the nominal problem, in order to solve this robust problem, we first solve the problems obtained by fixing N at $1, 2, \dots, N_{\max}$. For each fixed N , let $\vec{d}^*(N) = (d_1^*(N), \dots, d_N^*(N))$ denote the corresponding optimal dosing sequence. We then compare the objective values of these N dosing sequences and pick the best. Thus, the problem we need to solve for each fixed $N \in \{1, 2, \dots, N_{\max}\}$ is given by

$$\text{(RFRAC(N))} \quad f^*(N) = \max_{\vec{d}} \alpha_0 \sum_{t=1}^N d_t + \beta_0 \sum_{t=1}^N d_t^2 - \tau(N) \quad (23)$$

$$\sum_{t=1}^N d_t + \rho_m^{\text{mean}} \sum_{t=1}^N d_t^2 + \rho_m^{\text{range}} \left| \sum_{t=1}^N d_t^2 - \frac{D_m^2}{N_m} \right| \leq \text{RC}_m, \quad m \in \mathcal{M}, \quad (24)$$

$$\vec{d} \geq 0. \quad (25)$$

Note that when $\rho_m^{\min} = \rho_m^{\max} = \rho_m$, for $m = 1, 2, \dots, n$, that is, when there is no uncertainty in these dose-response parameters, (RFRAC(N)) reduces to the nominal QCQP (FRAC) with N fixed as presented in Section 1, and which was solved recently as a two-variable LP in [23, 26]. Note, however, that the objective function as well as the constraints in (RFRAC(N)) are non-convex, and the problem is at least as hard as the nominal QCQP. The objective function in the nominal QCQP is identical in form to what we have in (RFRAC(N)), but the convex, quadratic constraints in the nominal QCQP do not include the absolute value term that appears in the corresponding constraints in (RFRAC(N)). Specifically, it is this absolute value term that makes the robust counterpart harder to solve as compared to the nominal problem. To overcome this challenge, we decompose the feasible region of (RFRAC(N)) into $n+1$ subregions in a way such that the problem over each subregion can be solved via a two-variable LP. The details of this procedure are discussed in the next section.

3 Optimal solution of the robust formulation

To handle the absolute value term on the left hand side in constraints (24), we decompose the non-negative orthant $\{\vec{d} \in \mathbb{R}^N \mid \vec{d} \geq 0\}$ as follows. For each OAR $m \in \mathcal{M}$, consider two possibilities: the first is where $\sum_{t=1}^N d_t^2 \geq D_m^2/N_m$ and the second is $\sum_{t=1}^N d_t^2 < D_m^2/N_m$. Suppose, in the rest of this section, without loss of generality that $D_1^2/N_1 \leq D_2^2/N_2 \leq \dots \leq D_n^2/N_n$. Then, if there is a $\vec{d} \geq 0$ and an OAR $m \in \mathcal{M}$ such that $\sum_{t=1}^N d_t^2 \geq D_m^2/N_m$, then for this \vec{d} , we have that $\sum_{t=1}^N d_t^2 \geq D_{m'}^2/N_{m'}$

for all $m' < m$. Similarly, if there is a $\vec{d} \geq 0$ and an OAR $m \in \mathcal{M}$ such that $\sum_{t=1}^N d_t^2 < D_m^2/N_m$,

then for this \vec{d} , we have that $\sum_{t=1}^N d_t^2 < D_{m'}^2/N_{m'}$ for all $m' > m$. This means that the non-negative orthant $\{\vec{d} \in \mathbb{R}^N | \vec{d} \geq 0\}$ is partitioned into $n + 1$ subregions indexed by $k = 0, 1, 2, \dots, n$. In the k th region, $\sum_{t=1}^N d_t^2 \geq D_m^2/N_m$ for the **first** k OAR and $\sum_{t=1}^N d_t^2 < D_m^2/N_m$ for the **last** $n - k$ OAR.

Let $\text{RC}^+ = D_m + \rho_m^{\max} \frac{D_m^2}{N_m}$ and $\text{RC}^- = D_m + \rho_m^{\min} \frac{D_m^2}{N_m}$. Then, simple algebra reveals that for all \vec{d} in the k th subregion, constraint (24) reduces to $\sum_{t=1}^N d_t + \rho_m^{\max} \sum_{t=1}^N d_t^2 \leq \text{RC}_m^+$ for OAR $m = 1, 2, \dots, k$

when $k \neq 0$; and it reduces to $\sum_{t=1}^N d_t + \rho_m^{\min} \sum_{t=1}^N d_t^2 \leq \text{RC}_m^-$ for OAR $k + 1, k + 2, \dots, n$ when $k \neq n$.

As a result of the above discussion, (RFRAC(N)) is solved by solving $n + 1$ subproblems and then picking a dosing schedule with the largest tumor BE from the resulting $n + 1$ solutions. The k th subproblem is given by

$$(\text{kSub(N)}) \max_{\vec{d}} \alpha_0 \sum_{t=1}^N d_t + \beta_0 \sum_{t=1}^N d_t^2 - \tau(N) \quad (26)$$

$$\sum_{t=1}^N d_t + \rho_m^{\max} \sum_{t=1}^N d_t^2 \leq \text{RC}_m^+, \quad m = 1, 2, \dots, k, \quad k \neq 0, \quad (27)$$

$$\sum_{t=1}^N d_t + \rho_m^{\min} \sum_{t=1}^N d_t^2 \leq \text{RC}_m^-, \quad m = k + 1, k + 2, \dots, n, \quad k \neq n, \quad (28)$$

$$\sum_{t=1}^N d_t^2 \geq \frac{D_m^2}{N_m}, \quad m = 1, 2, \dots, k, \quad k \neq 0, \quad (29)$$

$$\sum_{t=1}^N d_t^2 < \frac{D_m^2}{N_m}, \quad m = k + 1, k + 2, \dots, n, \quad k \neq n, \quad (30)$$

$$\vec{d} \geq 0. \quad (31)$$

In addition, owing to the fact that $D_1^2/N_1 \leq D_2^2/N_2 \leq \dots \leq D_n^2/N_n$, the group of n constraints in (29)-(30) reduces to at most two constraints: $\sum_{t=1}^N d_t^2 \geq \frac{D_k^2}{N_k}$ when $k \neq 0$ and $\sum_{t=1}^N d_t^2 < \frac{D_{k+1}^2}{N_{k+1}}$ when $k \neq n$. After replacing this second strict inequality with a non-strict inequality¹, this simplifies the k th subproblem to

$$(\text{kSub(N)}) f^*(N; k) = \max_{\vec{d}} \alpha_0 \sum_{t=1}^N d_t + \beta_0 \sum_{t=1}^N d_t^2 - \tau(N) \quad (32)$$

$$\sum_{t=1}^N d_t + \rho_m^{\max} \sum_{t=1}^N d_t^2 \leq \text{RC}_m^+, \quad m = 1, 2, \dots, k, \quad k \neq 0, \quad (33)$$

¹This can be rigorously justified by proving that if there is a feasible dosing schedule that satisfies $\sum_{t=1}^N d_t^2 = \frac{D_{k+1}^2}{N_{k+1}}$ in the k th subproblem with a non-strict inequality, then this dosing schedule is feasible to the $k + 1$ st subproblem with a strict inequality; consequently, using non-strict inequalities does not alter optimality in our overall group of $n + 1$ subproblems with strict inequalities. We omit the details of this proof for brevity.

$$\sum_{t=1}^N d_t + \rho_m^{\min} \sum_{t=1}^N d_t^2 \leq \text{RC}_m^-, \quad m = k+1, k+2, \dots, n, \quad k \neq n, \quad (34)$$

$$\sum_{t=1}^N d_t^2 \geq \frac{D_k^2}{N_k}, \quad k \neq 0, \quad (35)$$

$$\sum_{t=1}^N d_t^2 \leq \frac{D_{k+1}^2}{N_{k+1}}, \quad k \neq n, \quad (36)$$

$$\vec{d} \geq 0. \quad (37)$$

The objective function and the constraints (33)-(34) in this subproblem are identical in form to that in the nominal problem (FRAC) with N fixed. Thus, the only difference between this subproblem and the nominal problem is the appearance of the additional constraints (35)-(36). In order to solve this problem, we first relax these two constraints and use the variable transformation $x = \sum_{t=1}^N d_t$ and $y = \sum_{t=1}^N d_t^2$ as in [23, 26], to convert the relaxed subproblem into an equivalent two-variable LP. To write this LP compactly, we first introduce additional notation. Let

$$\text{RC}_m^k = \begin{cases} \text{RC}_m^+, & \text{for } m = 1, 2, \dots, k, \quad k \neq 0, \\ \text{RC}_m^-, & \text{for } m = k+1, k+2, \dots, n, \quad k \neq n; \end{cases} \quad (38)$$

and similarly,

$$\rho_m^k = \begin{cases} \rho_m^{\max}, & \text{for } m = 1, 2, \dots, k, \quad k \neq 0, \\ \rho_m^{\min}, & \text{for } m = k+1, k+2, \dots, n, \quad k \neq n. \end{cases} \quad (39)$$

Moreover, let

$$c_k = \min_{m \in \mathcal{M}} \frac{-1 + \sqrt{1 + 4\rho_m^k \text{RC}_m^k / N}}{2\rho_m^k}, \quad \text{and} \quad (40)$$

$$\gamma_k = \min_{m \in \mathcal{M}} \frac{-1 + \sqrt{1 + 4\rho_m^k \text{RC}_m^k}}{2\rho_m^k}. \quad (41)$$

Then, the two-variable LP can be written as

$$(2\text{VARLPkSub}(N)) \quad \max_{x,y} \quad \alpha_0 x + \beta_0 y - \tau(N) \quad (42)$$

$$x + \rho_m^k y \leq \text{RC}_m^k, \quad m \in \mathcal{M}, \quad (43)$$

$$y \leq \gamma_k x, \quad (44)$$

$$c_k x \leq y, \quad (45)$$

$$x \geq 0, \quad (46)$$

$$y \geq 0. \quad (47)$$

Let x^*, y^* be an optimal solution to this two-variable LP. If $\frac{D_k^2}{N_k} \leq y^* \leq \frac{D_{k+1}^2}{N_{k+1}}$ as required by constraints (35)-(36), we are done. If not, then an optimal solution can be recovered as explained in Figure 1. Then, finally, a corresponding dosing schedule $\vec{d}^*(N) = (d_1^*(N), d_2^*(N), \dots, d_N^*(N)) = (q, \underbrace{p, p, \dots, p}_{N-1 \text{ times}})$ that is optimal to problem (kSub(N)) is recovered by formulas (12)-(13).

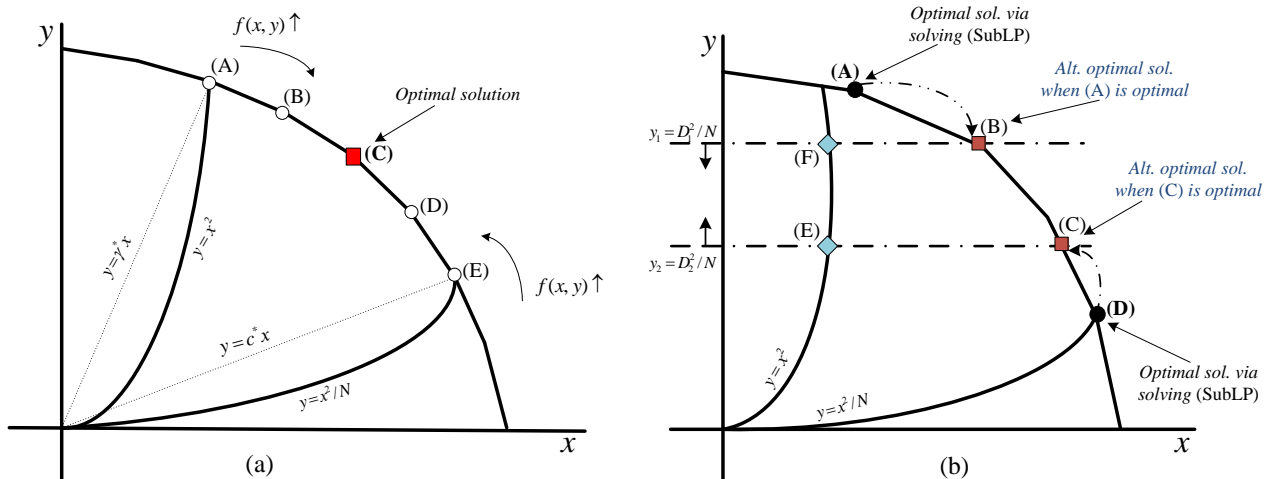


Figure 1: (a) A schematic illustration of the relationship between adjacent points in the feasible region of the subproblem k . When (C) is optimal, due to the linearity of the constraint and the objective function, it can be easily shown (via geometric or analytical proof) that the denoted points in the left-hand and right-hand side of the optimal point (C) are ranked as follows in terms of their objective value: $(A) \preceq (B) \preceq (C)$ and similarly, $(E) \preceq (D) \preceq (C)$. (b) A schematic illustration of the method for deriving the alternative optimal solution when optimal solution obtained by solving the relaxed subproblem (SubLP) does not belong to the feasible region of subproblem k . By following the same logic as in (a), we can argue that when (A) or (D) are the primary optimal solutions and are cut off by y_1 or y_2 , (B) or (C) are the next-best optimal solutions, respectively. Also, because of the slope of the objective function, (B) and (C) are superior to (F) and (E), respectively.

4 Numerical experiments

4.1 Qualitative properties of robust solutions

An unavoidable downside to using robust optimization in general is that it sacrifices the value of the objective function in favor of a robust solution. Thus, it is important to quantify how much we are losing in terms of the objective value by solving the robust problem instead of solving the nominal problem. This is often called the price of robustness.

In this section, we numerically quantify the price of robustness via computer simulations for head-and-neck cancer. In these simulations, as in [24], we considered four OAR ($n = 4$), namely, spinal cord, brainstem, left and right parotids. For the tumor, we fixed $\alpha_0 = 0.35 \text{ Gy}^{-1}$ and $\beta_0 = 0.035 \text{ Gy}^{-2}$ as is standard in the clinical literature [9, 10, 11, 12]. Again, based on the clinical literature [9, 11, 29], the nominal α/β ratios for spinal cord, brainstem, left and right parotids were fixed at 3, 4, 5, 6 Gy; that is, $\rho_1 = 1/3, \rho_2 = 1/4, \rho_3 = 1/5, \rho_4 = 1/6$. Here, we used different values of nominal ratios for different OAR to fully explore the various possibilities that could arise in a robust formulation with multiple OAR. The tolerance doses for these OAR were fixed at 45, 50, 26, and 28 Gy, respectively, and the conventional number of fractions N_m was fixed at 35 days for all OAR similar to the standard QUANTEC treatment protocol [19]. N_{\max} was set to 100 days. The uncertainty intervals were parameterized as $\tilde{\rho}_m \in [(1 - \delta)\rho_m, (1 + \delta)\rho_m]$, where $\delta \in [0, 1]$. This allowed us to easily quantify the price of robustness as a function of the uncertainty level δ . We varied δ from 0 (to represent the nominal case) to 1 (to denote the most uncertain case with 100% uncertainty) in increments of 0.1. All experiments were carried out in MATLAB on a laptop with 2.20 GHz Intel Core2 Duo CPU and 2 GB of memory, running a Microsoft Windows 8.1 operating system. Tables 1 and 2 summarize the results of our experiments for different values of $T_{\text{lag}}, T_{\text{double}}$, and δ . In these tables, T_{lag} values were set to 7, 14, 21, 28, 35 days based on [11] and T_{double} values were set to 2, 8, 10, 20, 40, 50, 80, 100 days based on [9, 11, 21, 29]. We are aware that the value of

35 days for T_{lag} is perhaps too high; similarly, the values of 80 and 100 days for T_{double} are also perhaps too high for head-and-neck cancer. These somewhat extreme values were included in our simulations to fully explore possible trends in various results of interest.

Table 1 shows, as expected, that the price of robustness increases with increasing δ for each T_{lag} , T_{double} combination. Overall, the price of robustness seems to be quite small in most experiments with an average of 1.27% over all 400 experiments. The first, second, and third quartiles were 0.12%, 0.47%, and 1.44%, respectively.

For each T_{lag} , δ combination in Table 1, the price of robustness first decreases with increasing T_{double} , reaches the smallest value when $T_{\text{double}} = 50$ days and then increases. This trend is consistent with the corresponding trend in the difference between $N_m = 35$ and N^* that can be inferred from Table 2. Specifically, for each T_{lag} , δ combination, the magnitude of $N_m - N^*$ decreases with increasing T_{double} , reaches about a day or two when $T_{\text{double}} = 50$, and then increases. In fact, as we can see in Figure 2(d), when $N = N_m = 35$, the price of robustness is exactly zero; more strongly, we found that this held true irrespective of the values of δ , T_{lag} , and T_{double} . A detailed algebraic proof of this fact can be developed, but is omitted here for brevity. Roughly speaking, the key idea in this proof is that when $N = N_m$, the BED constraints reduce to total dose constraints; this eliminates the dependence of the BED constraint on ρ_m and hence an equal-dosage solution that splits the tolerance dose across N fractions is optimal to the nominal *and* the robust problem. Consequently, the price of robustness is zero. Finally, for any combination of δ and T_{double} in Table 1, the price of robustness decreases as T_{lag} increases. Again, this is also consistent with the corresponding trend in the magnitude of $N_m - N^*$.

A closer look at Table 2 reveals that the evolution of N^* with δ for various fixed combinations of T_{double} and T_{lag} does not exhibit a universal trend. For instance, when $T_{\text{lag}} = 7$ days and $T_{\text{double}} = 2$ days, $N^* = 8$ for all δ (also see Figure 2 (a)). However, N^* increases with increasing δ when $T_{\text{lag}} = 7$ days and $T_{\text{double}} = 10$ days (Figure 2 (b)). On the other hand, N^* decreases as δ increases when $T_{\text{lag}} = 7$ days and $T_{\text{double}} = 100$ days (Figure 2 (c)). Consistent with this observation, Table 2 also shows that for each fixed combination of T_{double} and T_{lag} , optimal doses do not exhibit a universal qualitative trend as a function of δ .

Finally, our robust solutions continue to exhibit qualitative trends that are well-established in the nominal case (see [24] and references therein). For instance, N^* increases with increasing T_{double} for any fixed δ , T_{lag} combination; similarly, N^* also increases as T_{lag} increases for any fixed δ , T_{double} combination.

4.2 Infeasibility tests

As mentioned before, the primary motivation for the robust formulation is that the optimal solution obtained by solving the nominal formulation is guaranteed to be feasible only for nominal values of ρ . This means that if the actual ρ values turn out to be different than the nominal, the nominal solution might become infeasible. To quantify the frequency and extent of such infeasibility, we first performed a set of numerical experiments where the realized values of ρ were assumed to equal various grid-points in the uncertainty intervals around the nominal values. It turned out that while ρ varied in this manner over grid-points inside the uncertainty interval, the nominal solution was infeasible in about 75% of the cases; the robust solution of course remained feasible in all cases. The amount of infeasibility in some cases was rather large — close to 50%, with an average of 10.5%. The first, second, and third quartiles were 3.99%, 8.44%, and 15.76%, respectively. Given the relatively small price of robustness reported in Section 4.1, this suggests that it might be worthwhile to implement the robust dosing schedules rather than the nominal ones.

In the robust counterpart, we assumed that the value of ρ for each OAR belongs to a known

interval. Therefore, any solution to our robust formulation is guaranteed to be feasible only as long as this assumption holds. Due to the uncertainty in the actual values of ρ , however, this assumption could be violated. In that case, our robust solution might not be feasible after all. To test the impact of this unfortunate occurrence, we performed numerical experiments where ρ values were varied outside the predetermined uncertainty interval. In particular, for each uncertainty level δ and constraint m , five grid-points were chosen at $\tilde{\rho}^m = (1 + \delta + \gamma)\rho^m$ and five grid-points at $\tilde{\rho}^m = (1 - \delta - \gamma)\rho^m$, where $\gamma \in \{0.1, 0.2, \dots, 0.5\}$ and ρ^m denotes the nominal value. The nominal solution was infeasible in over 65% of the cases, while the robust solution was infeasible in 43% of the cases. The amount of infeasibility was found to be statistically lower (via a pairwise t-test at the $p = 0.05$ significance level) for the robust solution than the nominal solution over all cases. This is encouraging because it suggests that the robust solution might be “more robust” than the nominal solution even when ρ values are outside the uncertainty intervals (although it does not appear possible to rigorously state and prove this claim).

4.3 Uncertainty in tumor parameters

Throughout this paper, we assumed that the values of the tumor parameters α_0 and β_0 were known. In this section, we investigate the effect of uncertainty in these tumor parameters. We assume that both $\tilde{\alpha}_0$ and $\tilde{\beta}_0$ belong to a known interval. That is, $\tilde{\alpha}_0 \in [\alpha_0^{\min}, \alpha_0^{\max}]$ and $\tilde{\beta}_0 \in [\beta_0^{\min}, \beta_0^{\max}]$. Since we are maximizing the objective function, the worst realization of the problem occurs when $\tilde{\alpha}_0 = \alpha_0^{\min}$, $\tilde{\beta}_0 = \beta_0^{\min}$. That is, the robust objective value is simply attained by replacing $\tilde{\alpha}_0$ and $\tilde{\beta}_0$ by their minimum values. Table 3 shows the effect of this uncertainty, assuming that $\tilde{\alpha}_0 \in [(1 - \theta)\hat{\alpha}_0, (1 + \theta)\hat{\alpha}_0]$ and $\tilde{\beta}_0 \in [(1 - \theta)\hat{\beta}_0, (1 + \theta)\hat{\beta}_0]$. Here, the nominal values $\hat{\alpha}_0$ and $\hat{\beta}_0$ were set to 0.35 Gy and 0.035 Gy⁻², respectively, and θ was varied in the set $\{0.1, 0.2, \dots, 0.9\}$. A quick inspection of the table reveals that as the tumor uncertainty level increases, the number of fractions decreases and the dose delivered in each session increases. In other words, higher uncertainty in tumor parameters causes it to behave similar to faster-proliferating tumors.

5 Discussion

Most existing research on robust optimization in cancer radiotherapy focuses on incorporating uncertainty in the actual dose delivered to various anatomical regions of interest via intensity modulated radiation therapy (IMRT) and other treatment methods. Causes of this uncertainty include patient movement, say due to breathing, or setup errors at the time of treatment delivery (see, for instance, [6, 8, 16, 17, 18, 27] and references therein).

In this paper, we provided a robust formulation of the fractionation problem. Perhaps more importantly, we also described in detail a simple method for exact solution of this robust formulation. Although our robust formulation is, at first glance, inevitably at least as hard as a non-convex QCQP, we were able to show that it can be solved to optimality by solving a few two-variable LPs with a few constraints each. Our numerical experiments provided insights into the behavior of nominal and robust dosing schedules and also quantified the price of robustness. Overall, our comparison of the frequency and amount of infeasibility incurred by the nominal and the robust solutions suggests that the robust solutions are indeed statistically more feasible and yet pay a relatively small price of robustness. This could provide motivation for future investigations into the use of biological dose-response models such as the LQ model for planning radiation treatment as the uncertainty in dose-response parameters has been the main obstacle in widespread reliance on these models (see [14]).

Note that the nominal fractionation model in [24, 26] used the concept of sparing factors to model the doses delivered to the various OAR. For instance, if dose d_t is given to the tumor in fraction t , then the dose to OAR $m \in \mathcal{M}$ equals $s_m d_t$; here, s_m is a non-negative sparing factor. In this paper, we did not use such sparing factors because they would have been distracting to the main message of our work. We do emphasize, however, that our solution procedure in Section 3 would work even if such sparing factors were included. More strongly, our solution method would work even if the true values of these sparing factors were unknown but were instead assumed to belong to a non-negative interval. This can be done simply by using the largest values of these sparing factors in our robust formulation as in [1].

In a recent unpublished manuscript based on the doctoral dissertation of Saberian [23], Saberian et al. [25] presented a spatiotemporally integrated formulation of the fractionation problem. The decision variables in that formulation were N and the intensity profiles of the IMRT radiation fields employed in each fraction. The numbers of variables and constraints in that non-convex formulation are as large as tens of thousands. It would be interesting in the future to formulate the robust counterpart of that model and to devise efficient approximate solution methods.

6 Acknowledgment

Funded in part by the National Science Foundation through grant #CMMI 1054026.

References

- [1] H Badri, Y Watanabe, and K Leder. Robust and probabilistic optimization of dose schedules in radiotherapy. available online at arxiv.org/pdf/1503.00399v2.pdf, June 2015.
- [2] H Badri, Y Watanabe, and K Leder. Robust optimization of dose schedules in radiotherapy. available online at arxiv.org/pdf/1503.00399v1.pdf, March 2015.
- [3] A Ben-Tal, L El Ghaoui, and A Nemirovski. *Robust Optimization*. Princeton University Press, Princeton, NJ, USA, 2009.
- [4] D Bertsimas, D B Brown, and C Caramanis. Theory and applications of robust optimization. *SIAM Review*, 53(3):464–501, 2011.
- [5] A Bertuzzi, C Bruni F Papa, and C Sinisgalli. Optimal solution for a cancer radiotherapy problem. *Journal of Mathematical Biology*, 66(1-2):311–349, 2013.
- [6] T Bortfeld, T C Y Chan, A Trofimov, and J N Tsitsiklis. Robust management of motion uncertainty in intensity modulated radiation therapy. *Operations Research*, 56(6):1461–1473, 2008.
- [7] T Bortfeld, J Ramakrishnan, J N Tsitsiklis, and J Unkelbach. Optimization of radiotherapy fractionation schedules in the presence of tumor repopulation. forthcoming in INFORMS Journal on Computing, preprint available at http://pages.discovery.wisc.edu/~jramakrishnan/BRT2015_repop.pdf, May 2015.
- [8] T C Y Chan, T Bortfeld, and J Tsitsiklis. A robust approach to IMRT optimization. *Physics in Medicine and Biology*, 51:2567–2583, 2006.

- [9] J F Fowler. How worthwhile are short schedules in radiotherapy?: A series of exploratory calculations. *Radiotherapy and Oncology*, 18(2):165–181, 1990.
- [10] J F Fowler. Biological factors influencing optimum fractionation in radiation therapy. *Acta Oncologica*, 40(6):712–717, 2001.
- [11] J F Fowler. Is there an optimal overall time for head and neck radiotherapy? a review with new modeling. *Clinical Oncology*, 19(1):8–27, 2007.
- [12] J F Fowler. Optimum overall times II: Extended modelling for head and neck radiotherapy. *Clinical Oncology*, 20(2):113–126, 2008.
- [13] J F Fowler and M A Ritter. A rationale for fractionation for slowly proliferating tumors such as prostatic adenocarcinoma. *International Journal of Radiation Oncology Biology Physics*, 32(2):521–529, 1995.
- [14] E J Hall and A J Giaccia. *Radiobiology for the Radiologist*. Lippincott Williams & Wilkins, Philadelphia, Pennsylvania, USA, 2005.
- [15] B Jones, L T Tan, and R G Dale. Derivation of the optimum dose per fraction from the linear quadratic model. *The British Journal of Radiology*, 68(812):894–902, 1995.
- [16] H Mahmoudzadeh, J Lee, T C Y Chan, and T G Purdie. Robust optimization methods for cardiac sparing in tangential breast IMRT. *Medical Physics*, 42(5):2212, 2015.
- [17] H Mahmoudzadeh, T G Purdie, and T C Y Chan. Constraint generation methods for robust optimization in radiation therapy. forthcoming in *Operations Research for Health Care*, June 2015.
- [18] P A Mar and T C Y Chan. Adaptive and robust radiation therapy in the presence of drift. *Physics in Medicine and Biology*, 60(9):3599–3615, 2015.
- [19] L B Marks, E D Yorke, A Jackson, R K Ten Haken, L S Constine, A Eisbruch, S M Bentzen, J Nam, and J O Deasy. Use of normal tissue complication probability models in the clinic. *International Journal of Radiation Oncology Biology Physics*, 76(3):S10–S19, 2010.
- [20] M Mizuta, S Takao, H Date, N Kishimoto, K L Sutherland, R Onimaru, and H Shirato. A mathematical study to select fractionation regimen based on physical dose distribution and the linear-quadratic model. *International Journal of Radiation Oncology Biology Physics*, 84(3):829 – 833, 2012.
- [21] X S Qi, Q Yang, S P Lee, X A Li, and D Wang. An estimation of radiobiological parameters for head-and-neck cancer cells and the clinical implications. *Cancers*, 4:566–580, 2012.
- [22] S Rockwell. Experimental radiotherapy: a brief history. *Radiation Research*, 150(Supplement):S157–S169, November 1998.
- [23] F Saberian. *Convex and Dynamic Optimization with Learning for Adaptive Biologically Conformal Radiotherapy*. unpublished doctoral dissertation, University of Washington, Industrial and Systems Engineering, May 2015.
- [24] F Saberian, A Ghate, and M Kim. Optimal fractionation in radiotherapy with multiple normal tissues. forthcoming in *Mathematical Medicine and Biology*, online preprint available at doi: 10.1093/imammb/dqv015, May 2015.

- [25] F Saberian, A Ghate, and M Kim. Spatiotemporally integrated fractionation in radiotherapy. under review at INFORMS Journal on Computing, preprint available at <http://faculty.washington.edu/archis/upaper-apr-2015.pdf>, April 2015.
- [26] F Saberian, A Ghate, and M Kim. A two-variable linear program solves the standard linear–quadratic formulation of the fractionation problem in cancer radiotherapy. *Operations Research Letters*, 43(3):254 – 258, 2015.
- [27] J Unkelbach, T C Y Chan, and T Bortfeld. Accounting for range uncertainties in the optimization of intensity modulated proton therapy. *Physics in Medicine and Biology*, 52:2755–2773, 2007.
- [28] J Unkelbach, D Craft, E Saleri, J Ramakrishnan, and T Bortfeld. The dependence of optimal fractionation schemes on the spatial dose distribution. *Physics in Medicine and Biology*, 58(1):159–167, 2013.
- [29] Y Yang and L Xing. Optimization of radiotherapy dose-time fractionation with consideration of tumor specific biology. *Medical Physics*, 32(12):3666–3677, 2005.

$T_{\text{lag}} = 7$	T_{double}							
δ	2	8	10	20	40	50	80	100
0.1	1.74%	1.44%	1.21%	0.56%	0.04%	0.01%	0.25%	0.36%
0.2	3.34%	2.67%	2.23%	0.98%	0.04%	0.01%	0.39%	0.62%
0.3	4.80%	3.74%	3.10%	1.31%	0.04%	0.01%	0.39%	0.70%
0.4	6.14%	4.66%	3.85%	1.56%	0.04%	0.01%	0.39%	0.70%
0.5	7.38%	5.48%	4.51%	1.74%	0.04%	0.01%	0.39%	0.70%
0.6	8.53%	6.22%	5.09%	1.87%	0.04%	0.01%	0.39%	0.70%
0.7	9.61%	6.88%	5.61%	1.95%	0.04%	0.01%	0.39%	0.70%
0.8	10.61%	7.47%	6.07%	2.00%	0.04%	0.01%	0.39%	0.70%
0.9	11.54%	8.01%	6.47%	2.02%	0.04%	0.01%	0.39%	0.70%
1	12.42%	8.50%	6.84%	2.02%	0.04%	0.01%	0.39%	0.70%
$T_{\text{lag}} = 14$	T_{double}							
δ	2	8	10	20	40	50	80	100
0.1	0.92%	0.92%	0.92%	0.54%	0.04%	0.01%	0.25%	0.36%
0.2	1.78%	1.78%	1.78%	0.96%	0.04%	0.01%	0.38%	0.61%
0.3	2.59%	2.59%	2.59%	1.28%	0.04%	0.01%	0.39%	0.70%
0.4	3.34%	3.34%	3.30%	1.52%	0.04%	0.01%	0.39%	0.70%
0.5	4.05%	4.05%	3.93%	1.69%	0.04%	0.01%	0.39%	0.70%
0.6	4.71%	4.71%	4.48%	1.82%	0.04%	0.01%	0.39%	0.70%
0.7	5.34%	5.34%	4.97%	1.90%	0.04%	0.01%	0.39%	0.70%
0.8	5.93%	5.89%	5.41%	1.95%	0.04%	0.01%	0.39%	0.70%
0.9	6.49%	6.41%	5.80%	1.96%	0.04%	0.01%	0.39%	0.70%
1	7.02%	6.87%	6.14%	1.96%	0.04%	0.01%	0.39%	0.70%
$T_{\text{lag}} = 21$	T_{double}							
δ	2	8	10	20	40	50	80	100
0.1	0.47%	0.47%	0.47%	0.47%	0.04%	0.01%	0.25%	0.36%
0.2	0.92%	0.92%	0.92%	0.88%	0.04%	0.01%	0.38%	0.61%
0.3	1.34%	1.34%	1.34%	1.19%	0.04%	0.01%	0.39%	0.69%
0.4	1.74%	1.74%	1.74%	1.42%	0.04%	0.01%	0.39%	0.69%
0.5	2.12%	2.12%	2.12%	1.60%	0.04%	0.01%	0.39%	0.69%
0.6	2.48%	2.48%	2.48%	1.72%	0.04%	0.01%	0.39%	0.69%
0.7	2.82%	2.82%	2.82%	1.80%	0.04%	0.01%	0.39%	0.69%
0.8	3.14%	3.14%	3.14%	1.85%	0.04%	0.01%	0.39%	0.69%
0.9	3.45%	3.45%	3.45%	1.86%	0.04%	0.01%	0.39%	0.69%
1	3.75%	3.75%	3.75%	1.86%	0.04%	0.01%	0.39%	0.69%
$T_{\text{lag}} = 28$	T_{double}							
δ	2	8	10	20	40	50	80	100
0.1	0.18%	0.18%	0.18%	0.18%	0.04%	0.01%	0.25%	0.36%
0.2	0.35%	0.35%	0.35%	0.35%	0.04%	0.01%	0.38%	0.61%
0.3	0.52%	0.52%	0.52%	0.52%	0.04%	0.01%	0.38%	0.69%
0.4	0.67%	0.67%	0.67%	0.67%	0.04%	0.01%	0.38%	0.69%
0.5	0.82%	0.82%	0.82%	0.82%	0.04%	0.01%	0.38%	0.69%
0.6	0.97%	0.97%	0.97%	0.94%	0.04%	0.01%	0.38%	0.69%
0.7	1.10%	1.10%	1.10%	1.02%	0.04%	0.01%	0.38%	0.69%
0.8	1.23%	1.23%	1.23%	1.07%	0.04%	0.01%	0.38%	0.69%

0.9	1.36%	1.36%	1.36%	1.08%	0.04%	0.01%	0.38%	0.69%
1	1.48%	1.48%	1.48%	1.08%	0.04%	0.01%	0.38%	0.69%
$T_{\text{lag}} = 35$	T_{double}							
δ	2	8	10	20	40	50	80	100
0.1	0.03%	0.03%	0.03%	0.03%	0.03%	0.03%	0.25%	0.36%
0.2	0.06%	0.06%	0.06%	0.06%	0.06%	0.06%	0.38%	0.61%
0.3	0.08%	0.08%	0.08%	0.08%	0.08%	0.09%	0.41%	0.69%
0.4	0.12%	0.12%	0.12%	0.12%	0.12%	0.12%	0.44%	0.72%
0.5	0.15%	0.15%	0.15%	0.15%	0.15%	0.15%	0.47%	0.76%
0.6	0.15%	0.15%	0.15%	0.15%	0.15%	0.15%	0.47%	0.76%
0.7	0.15%	0.15%	0.15%	0.15%	0.15%	0.15%	0.47%	0.76%
0.8	0.15%	0.15%	0.15%	0.15%	0.15%	0.15%	0.47%	0.76%
0.9	0.15%	0.15%	0.15%	0.15%	0.15%	0.15%	0.47%	0.76%
1	0.15%	0.15%	0.15%	0.15%	0.15%	0.15%	0.47%	0.76%

Table 1: The price of robustness for different combinations of T_{lag} , T_{double} , and δ . The price of robustness equals $(\frac{g^* - f^*}{g^*}) \times 100\%$, where f^* and g^* are the optimal values of the robust and the nominal formulations, respectively.

$T_{\text{lag}} = 7$		T_{double}									
δ	2	8	10	20	40	50	80	100			
0	(2.49, 8)	(2.10,10)	(1.82,12)	(1.20,20)	(0.80,32)	(0.71,37)	(0.55,49)	(0.49,56)			
0.1	(2.46, 8)	(1.93,11)	(1.69,13)	(1.11,22)	(0.74,35)	(0.74,35)	(0.62,43)	(0.55,49)			
0.2	(2.42, 8)	(1.79,12)	(1.59,14)	(1.02,24)	(0.74,35)	(0.74,35)	(0.71,37)	(0.63,42)			
0.3	(2.39, 8)	(1.67,13)	(1.49,15)	(0.96,26)	(0.74,35)	(0.74,35)	(0.74,35)	(0.74,35)			
0.4	(2.36, 8)	(1.65,13)	(1.41,16)	(0.92,27)	(0.74,35)	(0.74,35)	(0.74,35)	(0.74,35)			
0.5	(2.34, 8)	(1.55,14)	(1.34,17)	(0.87,29)	(0.74,35)	(0.74,35)	(0.74,35)	(0.74,35)			
0.6	(2.31, 8)	(1.46,15)	(1.27,18)	(0.82,31)	(0.74,35)	(0.74,35)	(0.74,35)	(0.74,35)			
0.7	(2.29, 8)	(1.45,15)	(1.21,19)	(0.80,32)	(0.74,35)	(0.74,35)	(0.74,35)	(0.74,35)			
0.8	(2.27, 8)	(1.38,16)	(1.21,19)	(0.76,34)	(0.74,35)	(0.74,35)	(0.74,35)	(0.74,35)			
0.9	(2.25, 8)	(1.31,17)	(1.16,20)	(0.74,35)	(0.74,35)	(0.74,35)	(0.74,35)	(0.74,35)			
1	(2.23, 8)	(1.30,17)	(1.11,21)	(0.74,35)	(0.74,35)	(0.74,35)	(0.74,35)	(0.74,35)			
$T_{\text{lag}} = 14$		T_{double}									
δ	2	8	10	20	40	50	80	100			
0	(1.53,15)	(1.53,15)	(1.53,15)	(1.20,20)	(0.80,32)	(0.71,37)	(0.55,49)	(0.49,56)			
0.1	(1.51,15)	(1.51,15)	(1.51,15)	(1.11,22)	(0.74,35)	(0.74,35)	(0.62,43)	(0.55,49)			
0.2	(1.50,15)	(1.50,15)	(1.50,15)	(1.02,24)	(0.74,35)	(0.74,35)	(0.71,37)	(0.63,42)			
0.3	(1.49,15)	(1.49,15)	(1.49,15)	(0.96,26)	(0.74,35)	(0.74,35)	(0.74,35)	(0.74,35)			
0.4	(1.48,15)	(1.48,15)	(1.41,16)	(0.92,27)	(0.74,35)	(0.74,35)	(0.74,35)	(0.74,35)			
0.5	(1.47,15)	(1.47,15)	(1.34,17)	(0.87,29)	(0.74,35)	(0.74,35)	(0.74,35)	(0.74,35)			
0.6	(1.46,15)	(1.46,15)	(1.27,18)	(0.82,31)	(0.74,35)	(0.74,35)	(0.74,35)	(0.74,35)			
0.7	(1.45,15)	(1.45,15)	(1.21,19)	(0.80,32)	(0.74,35)	(0.74,35)	(0.74,35)	(0.74,35)			
0.8	(1.45,15)	(1.38,16)	(1.21,19)	(0.76,34)	(0.74,35)	(0.74,35)	(0.74,35)	(0.74,35)			
0.9	(1.44,15)	(1.31,17)	(1.16,20)	(0.74,35)	(0.74,35)	(0.74,35)	(0.74,35)	(0.74,35)			
1	(1.43,15)	(1.30,17)	(1.11,21)	(0.74,35)	(0.74,35)	(0.74,35)	(0.74,35)	(0.74,35)			
$T_{\text{lag}} = 21$		T_{double}									
δ	2	8	10	20	40	50	80	100			
0	(1.11,22)	(1.11,22)	(1.11,22)	(1.11,22)	(0.80,32)	(0.71,37)	(0.55,49)	(0.49,56)			
0.1	(1.11,22)	(1.11,22)	(1.11,22)	(1.11,22)	(0.74,35)	(0.74,35)	(0.62,43)	(0.55,49)			
0.2	(1.10,22)	(1.10,22)	(1.10,22)	(1.02,24)	(0.74,35)	(0.74,35)	(0.71,37)	(0.63,42)			
0.3	(1.10,22)	(1.10,22)	(1.10,22)	(0.96,26)	(0.74,35)	(0.74,35)	(0.74,35)	(0.74,35)			
0.4	(1.09,22)	(1.09,22)	(1.09,22)	(0.92,27)	(0.74,35)	(0.74,35)	(0.74,35)	(0.74,35)			
0.5	(1.09,22)	(1.09,22)	(1.09,22)	(0.87,29)	(0.74,35)	(0.74,35)	(0.74,35)	(0.74,35)			
0.6	(1.09,22)	(1.09,22)	(1.09,22)	(0.82,31)	(0.74,35)	(0.74,35)	(0.74,35)	(0.74,35)			
0.7	(1.08,22)	(1.08,22)	(1.08,22)	(0.80,32)	(0.74,35)	(0.74,35)	(0.74,35)	(0.74,35)			
0.8	(1.08,22)	(1.08,22)	(1.08,22)	(0.76,34)	(0.74,35)	(0.74,35)	(0.74,35)	(0.74,35)			

	T_{double}									
	2	8	10	20	40	50	80	100		
0.9	(1.08,22)	(1.08,22)	(1.08,22)	(0.74,35)	(0.74,35)	(0.74,35)	(0.74,35)	(0.74,35)	(0.74,35)	(0.74,35)
1	(1.07,22)	(1.07,22)	(1.07,22)	(0.74,35)	(0.74,35)	(0.74,35)	(0.74,35)	(0.74,35)	(0.74,35)	(0.74,35)
$T_{\text{lag}} = 28$										
δ	2	8	10	20	40	50	80	100		
0	(0.88,29)	(0.88,29)	(0.88,29)	(0.88,29)	(0.80,32)	(0.71,37)	(0.55,49)	(0.49,56)		
0.1	(0.87,29)	(0.87,29)	(0.87,29)	(0.87,29)	(0.74,35)	(0.74,35)	(0.62,43)	(0.55,49)		
0.2	(0.87,29)	(0.87,29)	(0.87,29)	(0.87,29)	(0.74,35)	(0.74,35)	(0.71,37)	(0.63,42)		
0.3	(0.87,29)	(0.87,29)	(0.87,29)	(0.87,29)	(0.74,35)	(0.74,35)	(0.74,35)	(0.74,35)		
0.4	(0.87,29)	(0.87,29)	(0.87,29)	(0.87,29)	(0.74,35)	(0.74,35)	(0.74,35)	(0.74,35)		
0.5	(0.87,29)	(0.87,29)	(0.87,29)	(0.87,29)	(0.74,35)	(0.74,35)	(0.74,35)	(0.74,35)		
0.6	(0.87,29)	(0.87,29)	(0.87,29)	(0.82,31)	(0.74,35)	(0.74,35)	(0.74,35)	(0.74,35)		
0.7	(0.87,29)	(0.87,29)	(0.87,29)	(0.80,32)	(0.74,35)	(0.74,35)	(0.74,35)	(0.74,35)		
0.8	(0.87,29)	(0.87,29)	(0.87,29)	(0.76,34)	(0.74,35)	(0.74,35)	(0.74,35)	(0.74,35)		
0.9	(0.87,29)	(0.87,29)	(0.87,29)	(0.74,35)	(0.74,35)	(0.74,35)	(0.74,35)	(0.74,35)		
1	(0.86,29)	(0.86,29)	(0.86,29)	(0.74,35)	(0.74,35)	(0.74,35)	(0.74,35)	(0.74,35)		
$T_{\text{lag}} = 35$										
δ	2	8	10	20	40	50	80	100		
0	(0.72,36)	(0.72,36)	(0.72,36)	(0.72,36)	(0.72,36)	(0.71,37)	(0.55,49)	(0.49,56)		
0.1	(0.72,36)	(0.72,36)	(0.72,36)	(0.72,36)	(0.72,36)	(0.72,36)	(0.62,43)	(0.55,49)		
0.2	(0.72,36)	(0.72,36)	(0.72,36)	(0.72,36)	(0.72,36)	(0.72,36)	(0.71,37)	(0.63,42)		
0.3	(0.72,36)	(0.72,36)	(0.72,36)	(0.72,36)	(0.72,36)	(0.72,36)	(0.72,36)	(0.72,36)		
0.4	(0.72,36)	(0.72,36)	(0.72,36)	(0.72,36)	(0.72,36)	(0.72,36)	(0.72,36)	(0.72,36)		
0.5	(0.74,35)	(0.74,35)	(0.74,35)	(0.74,35)	(0.74,35)	(0.74,35)	(0.74,35)	(0.74,35)		
0.6	(1.44,0.70,36)*	(1.44,0.70,36)*	(1.44,0.70,36)*	(1.44,0.70,36)*	(1.44,0.70,36)*	(1.44,0.70,36)*	(1.44,0.70,36)*	(1.44,0.70,36)*		
0.7	(1.44,0.70,36)*	(1.44,0.70,36)*	(1.44,0.70,36)*	(1.44,0.70,36)*	(1.44,0.70,36)*	(1.44,0.70,36)*	(1.44,0.70,36)*	(1.44,0.70,36)*		
0.8	(0.74,35)	(0.74,35)	(0.74,35)	(0.74,35)	(0.74,35)	(0.74,35)	(0.74,35)	(0.74,35)		
0.9	(1.44,0.70,36)*	(1.44,0.70,36)*	(1.44,0.70,36)*	(1.44,0.70,36)*	(1.44,0.70,36)*	(1.44,0.70,36)*	(1.44,0.70,36)*	(1.44,0.70,36)*		
1	(1.44,0.70,36)*	(1.44,0.70,36)*	(1.44,0.70,36)*	(1.44,0.70,36)*	(1.44,0.70,36)*	(1.44,0.70,36)*	(1.44,0.70,36)*	(1.44,0.70,36)*		

Table 2: The optimal solution (d^*, N^*) of the robust and nominal models for different combinations of $T_{\text{lag}}, T_{\text{double}}$, and δ . The first row in each section of the table shows the solution of the nominal case ($\delta = 0$). The cases marked with an asterisk (*) yield unequal-dosage solutions characterized by two dose values (q, p) (recall formulas (12)-(13)) and an N^* value in that order.

$T_{double} = 8$									
θ									
$T_{tag} = 7$	0.1	0.2	0.3	0.4	0.5	0.6	0.7	0.8	0.9
δ									
0	(2.28, 9)	(2.49, 8)	(2.49, 8)	(2.49, 8)	(2.49, 8)	(2.49, 8)	(2.49, 8)	(2.49, 8)	(2.49, 8)
0.1	(2.08,10)	(2.25, 9)	(2.46, 8)	(2.46, 8)	(2.46, 8)	(2.46, 8)	(2.46, 8)	(2.46, 8)	(2.46, 8)
0.2	(1.91,11)	(2.05,10)	(2.22, 9)	(2.42, 8)	(2.42, 8)	(2.42, 8)	(2.42, 8)	(2.42, 8)	(2.42, 8)
0.3	(1.89,11)	(2.03,10)	(2.19, 9)	(2.39, 8)	(2.39, 8)	(2.39, 8)	(2.39, 8)	(2.39, 8)	(2.39, 8)
0.4	(1.75,12)	(1.87,11)	(2.01,10)	(2.36, 8)	(2.36, 8)	(2.36, 8)	(2.36, 8)	(2.36, 8)	(2.36, 8)
0.5	(1.64,13)	(1.74,12)	(1.99,10)	(2.15, 9)	(2.34, 8)	(2.34, 8)	(2.34, 8)	(2.34, 8)	(2.34, 8)
0.6	(1.63,13)	(1.73,12)	(1.84,11)	(2.13, 9)	(2.31, 8)	(2.31, 8)	(2.31, 8)	(2.31, 8)	(2.31, 8)
0.7	(1.53,14)	(1.62,13)	(1.83,11)	(1.96,10)	(2.29, 8)	(2.29, 8)	(2.29, 8)	(2.29, 8)	(2.29, 8)
0.8	(1.45,15)	(1.61,13)	(1.70,12)	(1.94,10)	(2.27, 8)	(2.27, 8)	(2.27, 8)	(2.27, 8)	(2.27, 8)
0.9	(1.44,15)	(1.51,14)	(1.69,12)	(1.93,10)	(2.25, 8)	(2.25, 8)	(2.25, 8)	(2.25, 8)	(2.25, 8)
1	(1.36,16)	(1.50,14)	(1.68,12)	(1.79,11)	(2.06, 9)	(2.23, 8)	(2.23, 8)	(2.23, 8)	(2.23, 8)

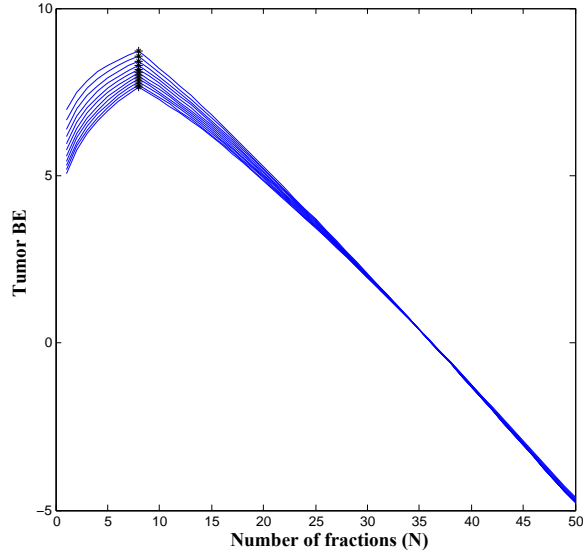
$T_{double} = 10$									
θ									
$T_{tag} = 7$	0.1	0.2	0.3	0.4	0.5	0.6	0.7	0.8	0.9
δ									
0	(1.95,11)	(2.10,10)	(2.28, 9)	(2.49, 8)	(2.49, 8)	(2.49, 8)	(2.49, 8)	(2.49, 8)	(2.49, 8)
0.1	(1.80,12)	(1.93,11)	(2.08,10)	(2.46, 8)	(2.46, 8)	(2.46, 8)	(2.46, 8)	(2.46, 8)	(2.46, 8)
0.2	(1.68,13)	(1.79,12)	(2.05,10)	(2.22, 9)	(2.42, 8)	(2.42, 8)	(2.42, 8)	(2.42, 8)	(2.42, 8)
0.3	(1.57,14)	(1.67,13)	(1.89,11)	(2.03,10)	(2.39, 8)	(2.39, 8)	(2.39, 8)	(2.39, 8)	(2.39, 8)
0.4	(1.48,15)	(1.65,13)	(1.75,12)	(2.01,10)	(2.17, 9)	(2.36, 8)	(2.36, 8)	(2.36, 8)	(2.36, 8)
0.5	(1.40,16)	(1.55,14)	(1.64,13)	(1.86,11)	(2.15, 9)	(2.34, 8)	(2.34, 8)	(2.34, 8)	(2.34, 8)
0.6	(1.39,16)	(1.46,15)	(1.63,13)	(1.84,11)	(1.97,10)	(2.31, 8)	(2.31, 8)	(2.31, 8)	(2.31, 8)
0.7	(1.32,17)	(1.45,15)	(1.53,14)	(1.71,12)	(1.96,10)	(2.29, 8)	(2.29, 8)	(2.29, 8)	(2.29, 8)
0.8	(1.26,18)	(1.38,16)	(1.52,14)	(1.70,12)	(1.94,10)	(2.27, 8)	(2.27, 8)	(2.27, 8)	(2.27, 8)
0.9	(1.25,18)	(1.31,17)	(1.44,15)	(1.60,13)	(1.80,11)	(2.25, 8)	(2.25, 8)	(2.25, 8)	(2.25, 8)
1	(1.20,19)	(1.30,17)	(1.43,15)	(1.59,13)	(1.79,11)	(2.06, 9)	(2.23, 8)	(2.23, 8)	(2.23, 8)

$T_{double} = 20$									
θ									
$T_{tag} = 7$	0.1	0.2	0.3	0.4	0.5	0.6	0.7	0.8	0.9
δ									
0	(1.31,18)	(1.38,17)	(1.53,15)	(1.61,14)	(1.82,12)	(2.10,10)	(2.49, 8)	(2.49, 8)	(2.49, 8)
0.1	(1.20,20)	(1.25,19)	(1.37,17)	(1.51,15)	(1.69,13)	(1.93,11)	(2.46, 8)	(2.46, 8)	(2.46, 8)
0.2	(1.10,22)	(1.19,20)	(1.30,18)	(1.43,16)	(1.59,14)	(1.79,12)	(2.22, 9)	(2.42, 8)	(2.42, 8)
0.3	(1.02,24)	(1.10,22)	(1.19,20)	(1.29,18)	(1.49,15)	(1.67,13)	(2.03,10)	(2.39, 8)	(2.39, 8)
0.4	(0.98,25)	(1.05,23)	(1.13,21)	(1.23,19)	(1.41,16)	(1.65,13)	(2.01,10)	(2.36, 8)	(2.36, 8)
0.5	(0.92,27)	(0.98,25)	(1.09,22)	(1.18,20)	(1.34,17)	(1.55,14)	(1.86,11)	(2.34, 8)	(2.34, 8)
0.6	(0.89,28)	(0.95,26)	(1.05,23)	(1.13,21)	(1.27,18)	(1.46,15)	(1.84,11)	(2.31, 8)	(2.31, 8)

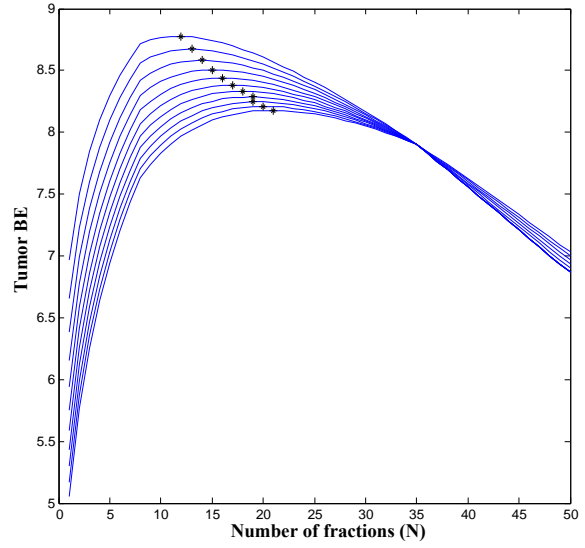
$T_{double} = 40$										
θ										
$T_{lag} = 7$	δ	0.1	0.2	0.3	0.4	0.5	0.6	0.7	0.8	0.9
0.7	(0.84,30)	(0.92,27)	(1.01,24)	(1.08,22)	(1.21,19)	(1.45,15)	(1.71,12)	(2.29, 8)	(2.29, 8)	(2.29, 8)
0.8	(0.82,31)	(0.89,28)	(0.95,26)	(1.04,23)	(1.21,19)	(1.38,16)	(1.70,12)	(2.27, 8)	(2.27, 8)	(2.27, 8)
0.9	(0.80,32)	(0.87,29)	(0.92,27)	(1.04,23)	(1.16,20)	(1.31,17)	(1.60,13)	(2.25, 8)	(2.25, 8)	(2.25, 8)
1	(0.78,33)	(0.82,31)	(0.89,28)	(1.00,24)	(1.11,21)	(1.30,17)	(1.59,13)	(2.06, 9)	(2.06, 9)	(2.23, 8)
$T_{double} = 50$										
θ										
$T_{lag} = 7$	δ	0.1	0.2	0.3	0.4	0.5	0.6	0.7	0.8	0.9
0	(0.85,30)	(0.93,27)	(1.00,25)	(1.07,23)	(1.20,20)	(1.38,17)	(1.61,14)	(2.10,10)	(2.10,10)	(2.49, 8)
0.1	(0.78,33)	(0.85,30)	(0.90,28)	(0.99,25)	(1.11,22)	(1.25,19)	(1.51,15)	(1.93,11)	(1.93,11)	(2.46, 8)
0.2	(0.74,35)	(0.78,33)	(0.85,30)	(0.93,27)	(1.02,24)	(1.19,20)	(1.43,16)	(1.79,12)	(1.79,12)	(2.42, 8)
0.3	(0.74,35)	(0.74,35)	(0.78,33)	(0.87,29)	(0.96,26)	(1.10,22)	(1.29,18)	(1.67,13)	(1.67,13)	(2.39, 8)
0.4	(0.74,35)	(0.74,35)	(0.74,35)	(0.82,31)	(0.92,27)	(1.05,23)	(1.23,19)	(1.65,13)	(1.65,13)	(2.36, 8)
0.5	(0.74,35)	(0.74,35)	(0.74,35)	(0.78,33)	(0.87,29)	(0.98,25)	(1.18,20)	(1.55,14)	(1.55,14)	(2.34, 8)
0.6	(0.74,35)	(0.74,35)	(0.74,35)	(0.74,35)	(0.82,31)	(0.95,26)	(1.13,21)	(1.46,15)	(1.46,15)	(2.31, 8)
0.7	(0.74,35)	(0.74,35)	(0.74,35)	(0.74,35)	(0.80,32)	(0.92,27)	(1.08,22)	(1.45,15)	(1.45,15)	(2.29, 8)
0.8	(0.74,35)	(0.74,35)	(0.74,35)	(0.74,35)	(0.76,34)	(0.89,28)	(1.04,23)	(1.38,16)	(1.38,16)	(2.27, 8)
0.9	(0.74,35)	(0.74,35)	(0.74,35)	(0.74,35)	(0.74,35)	(0.87,29)	(1.04,23)	(1.31,17)	(1.31,17)	(2.25, 8)
1	(0.74,35)	(0.74,35)	(0.74,35)	(0.74,35)	(0.74,35)	(0.82,31)	(1.00,24)	(1.30,17)	(1.30,17)	(2.06, 9)
$T_{double} = 80$										
θ										
$T_{lag} = 7$	δ	0.1	0.2	0.3	0.4	0.5	0.6	0.7	0.8	0.9
0	(0.76,34)	(0.80,32)	(0.88,29)	(0.96,26)	(1.07,23)	(1.20,20)	(1.45,16)	(1.82,12)	(1.82,12)	(2.49, 8)
0.1	(0.74,35)	(0.74,35)	(0.80,32)	(0.87,29)	(0.96,26)	(1.11,22)	(1.31,18)	(1.69,13)	(1.69,13)	(2.46, 8)
0.2	(0.74,35)	(0.74,35)	(0.74,35)	(0.80,32)	(0.90,28)	(1.02,24)	(1.24,19)	(1.59,14)	(1.59,14)	(2.42, 8)
0.3	(0.74,35)	(0.74,35)	(0.74,35)	(0.76,34)	(0.85,30)	(0.96,26)	(1.14,21)	(1.49,15)	(1.49,15)	(2.39, 8)
0.4	(0.74,35)	(0.74,35)	(0.74,35)	(0.74,35)	(0.80,32)	(0.92,27)	(1.09,22)	(1.41,16)	(1.41,16)	(2.17, 9)
0.5	(0.74,35)	(0.74,35)	(0.74,35)	(0.74,35)	(0.76,34)	(0.87,29)	(1.05,23)	(1.34,17)	(1.34,17)	(2.15, 9)
0.6	(0.74,35)	(0.74,35)	(0.74,35)	(0.74,35)	(0.74,35)	(0.82,31)	(0.98,25)	(1.27,18)	(1.27,18)	(1.97,10)
0.7	(0.74,35)	(0.74,35)	(0.74,35)	(0.74,35)	(0.74,35)	(0.80,32)	(0.95,26)	(1.21,19)	(1.21,19)	(1.96,10)
0.8	(0.74,35)	(0.74,35)	(0.74,35)	(0.74,35)	(0.74,35)	(0.76,34)	(0.92,27)	(1.21,19)	(1.21,19)	(1.94,10)
0.9	(0.74,35)	(0.74,35)	(0.74,35)	(0.74,35)	(0.74,35)	(0.74,35)	(0.89,28)	(1.16,20)	(1.16,20)	(1.80,11)
1	(0.74,35)	(0.74,35)	(0.74,35)	(0.74,35)	(0.74,35)	(0.74,35)	(0.86,29)	(1.11,21)	(1.11,21)	(1.79,11)
$T_{double} = 80$										
θ										
$T_{lag} = 7$	δ	0.1	0.2	0.3	0.4	0.5	0.6	0.7	0.8	0.9
0	(0.58,46)	(0.62,43)	(0.67,39)	(0.72,36)	(0.80,32)	(0.93,27)	(1.07,23)	(1.38,17)	(1.38,17)	(2.10,10)
0.1	(0.66,40)	(0.69,38)	(0.74,35)	(0.74,35)	(0.74,35)	(0.85,30)	(0.99,25)	(1.25,19)	(1.25,19)	(1.93,11)
0.2	(0.74,35)	(0.74,35)	(0.74,35)	(0.74,35)	(0.74,35)	(0.78,33)	(0.93,27)	(1.19,20)	(1.19,20)	(1.79,12)

0.3	(0.74,35)	(0.74,35)	(0.74,35)	(0.74,35)	(0.74,35)	(0.74,35)	(0.74,35)	(0.74,35)	(0.74,35)	(0.87,29)	(1.10,22)	(1.67,13)
0.4	(0.74,35)	(0.74,35)	(0.74,35)	(0.74,35)	(0.74,35)	(0.74,35)	(0.74,35)	(0.74,35)	(0.74,35)	(0.82,31)	(1.05,23)	(1.65,13)
0.5	(0.74,35)	(0.74,35)	(0.74,35)	(0.74,35)	(0.74,35)	(0.74,35)	(0.74,35)	(0.74,35)	(0.74,35)	(0.78,33)	(0.98,25)	(1.55,14)
0.6	(0.74,35)	(0.74,35)	(0.74,35)	(0.74,35)	(0.74,35)	(0.74,35)	(0.74,35)	(0.74,35)	(0.74,35)	(0.74,35)	(0.95,26)	(1.46,15)
0.7	(0.74,35)	(0.74,35)	(0.74,35)	(0.74,35)	(0.74,35)	(0.74,35)	(0.74,35)	(0.74,35)	(0.74,35)	(0.74,35)	(0.92,27)	(1.45,15)
0.8	(0.74,35)	(0.74,35)	(0.74,35)	(0.74,35)	(0.74,35)	(0.74,35)	(0.74,35)	(0.74,35)	(0.74,35)	(0.74,35)	(0.89,28)	(1.38,16)
0.9	(0.74,35)	(0.74,35)	(0.74,35)	(0.74,35)	(0.74,35)	(0.74,35)	(0.74,35)	(0.74,35)	(0.74,35)	(0.74,35)	(0.87,29)	(1.31,17)
1	(0.74,35)	(0.74,35)	(0.74,35)	(0.74,35)	(0.74,35)	(0.74,35)	(0.74,35)	(0.74,35)	(0.74,35)	(0.74,35)	(0.82,31)	(1.30,17)

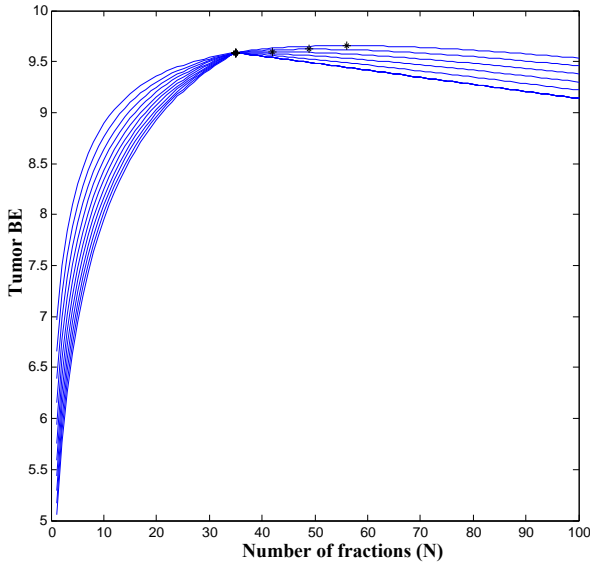
Table 3: Optimal dosage and optimal number of fractions (d^*, N^*) in the presence of uncertainty in tumor parameters (denoted by θ) and uncertainty in ρ parameters (denoted by δ).



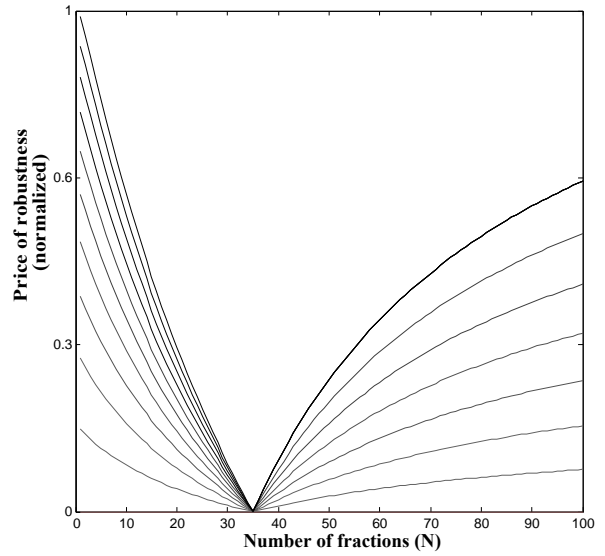
(a)



(b)



(c)



(d)

Figure 2: (a), (b), (c): The value of the objective as a function of N for $T_{\text{lag}} = 7$. The data points denoted by $*$ show the points (N^*, f^*) in each graph. The uppermost line in each set of graphs (a), (b), and (c) represents the nominal case ($\delta = 0$) and the other lines correspond to $\delta = \{0.1, 0.2, \dots, 1\}$, respectively, from top to bottom. (a) $T_{\text{double}} = 2$ days and $N^* = 8$ for all δ . (b) $T_{\text{double}} = 10$ days. In this case, N^* increases with increasing δ . (c) $T_{\text{double}} = 100$ days. In this case, N^* decreases with increasing δ (from top to bottom). Moreover, note that in some cases (for example in (c)), some of these points lie on top of each other as the optimal solution for their corresponding δ are equal. (d) Normalized price of robustness as a function of N when $T_{\text{lag}} = 7$, $T_{\text{double}} = 2$. The uppermost line represents the most uncertain case ($\delta = 1$) and other lines represent $\delta = \{0.9, 0.8, \dots, 0.1\}$, respectively, from top to bottom.